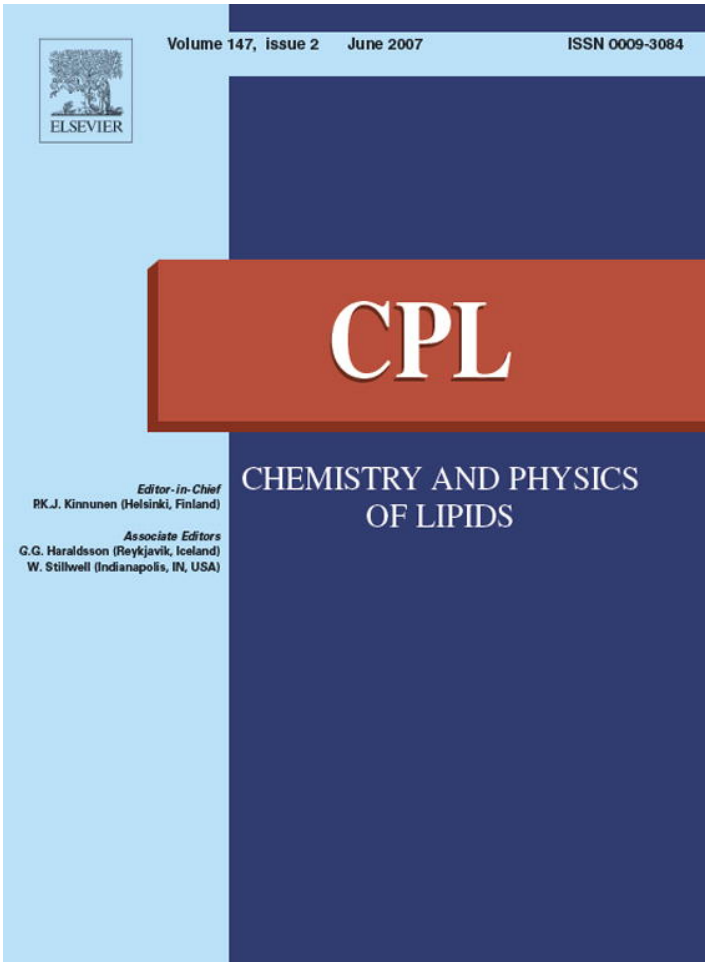

Available online at www.sciencedirect.com
ScienceDirect
Chemistry and Physics of Lipids 147 (2007) 69–77
CPL
CHEMISTRY AND PHYSICS OF LIPIDS
www.elsevier.com/locate/chemphyslip

Molecular interpretation of fluorescence solvent relaxation of Patman and ^{2}H NMR experiments in phosphatidylcholine bilayers

A. Olžyńska [a], A. Zań [a], P. Jurkiewicz [a], J. Sýkora [a], G. Gröbner [b], M. Langner [c], M. Hof [a,*]

[a] *Academy of Sciences of the Czech Republic, J. Heyrovský Institute of Physical Chemistry, v.v.i., Dolejškova 3, CZ-18223 Prague 8, Czech Republic*
[b] *Department of Biophysical Chemistry, Umeå University, 90187 Umeå, Sweden*
[c] *Institute of Physics, Wrocław University of Technology, Wybrzeże Wyspiańskiego 27, 50-370 Wrocław, Poland*

Received 5 December 2006; received in revised form 9 March 2007; accepted 14 March 2007
Available online 20 March 2007

Abstract

The analysis of time-dependent fluorescence shifts of the bilayer probe 6-hexadecanoyl-2-(((2-(trimethylammonium)ethyl) methyl)amino)naphthalene chloride (Patman) offers valuable information on the hydration and dynamics of phospholipid headgroups. Quenching studies on vesicles composed of four phosphatidylcholines with different hydrocarbon chains (18:1c9/18:1c9, DOPC; 16:0/18:1c9, POPC; 18:1c9/16:0, OPPC; 18:1c6/18:1c6, PCΔ6) show that the chromophore of Patman is defined located at the level of the *sn*-1 ester-group in the phospholipid, which is invariant to the hydrocarbon chain. The so-called solvent relaxation (SR) approach as well as solid-state ^{2}H NMR reveals that DOPC and PCΔ6 are more hydrated than POPC and OPPC. A strong dependence of SR kinetics on the position of double bond in the investigated fatty acid chains was observed. Apparently, the closer the double bond is located to the hydrated *sn*-1 ester-group, the more mobile this group becomes. This work demonstrates that the SR approach can report mobility changes within phospholipid bilayers with a remarkable molecular resolution.

Keywords: Solvent relaxation; ^{2}H NMR; Patman; Lipid hydration; Unsaturated hydrocarbon chain

1. Introduction

Fluorescence solvent relaxation has proved to be a powerful technique for studies of hydration and mobility of phospholipids headgroups (Jurkiewicz et al., 2005). This technique is based on the characterization of time-dependent shifts of fluorescence spectra of chromophores located at different depths within a phospholipid bilayer. In particular, 6-hexadecanoyl-2-(((2-(trimethylammonium)ethyl)methyl)amino)naphthalene chloride (Patman) was shown to reside at a well-defined location within the phospholipid region. The long hydrophobic palmitoyl tail of Patman anchors the molecule in the hydrophobic part of lipid bilayer while the attached trimethylammonium group serves to orient the alkylamino end of the fluorophore toward the lipid–water interface (Lakowicz et al., 1983) stabilizing the position of Patman in the bilayer due to interactions with charged phospholipid headgroups. Solvent relaxation data indicated that the time-dependent fluorescence shift of Patman in liquid-crystalline lipid

* Corresponding author. Tel.: +420 266053264; fax: +420 286582677.
E-mail address: martin.hof@jh-inst.cas.cz (M. Hof).

0009-3084/$ – see front matter © 2007 Elsevier Ireland Ltd. All rights reserved.
doi:10.1016/j.chemphyslip.2007.03.004

membrane occurring exclusively on the nanosecond timescale is related to the amount and mobility of bound water molecules located at the carbonyl region of the lipid bilayer (Hutterer et al., 1996; Sykora et al., 2002). In general, these shifts are interpreted in terms of collective mobility of bound water molecules together with the hydrated functional groups of the lipids (Hutterer et al., 1998; 1996; Nilsson and Halle, 2005). In the present study, we characterize the environment of Patman on a molecular level. Its localization along the *z*-axis of phosphatidylcholine bilayer is determined by quenching experiments. Based on this information, the solvent relaxation response was used to study the microenvironment probed by Patman in various bilayers formed by symmetric (1,2-dioleoyl-*sn*-glycero-3-phosphocholine (DOPC) and 1,2-dipetroselinoyl-*sn*-glycero-3-phosphocholine (PCΔ6)) or asymmetric (1,2-oleoyl-palmitoyl-*sn*-glycero-3-phosphocholine (OPPC) and 1,2-palmitoyl-oleoyl-*sn*-glycero-3-phosphocholine (POPC)) phosphatidylcholines. The solid-state ^{2}H NMR studies using D_2O to screen the inner hydration shells of the lipids, support the basic molecular view obtained by the solvent relaxation.

2. Materials and methods

2.1. Materials

1,2-Oleoyl-palmitoyl-*sn*-glycero-3-phosphocholine (OPPC), 1,2-palmitoyl-oleoyl-*sn*-glycero-3-phosphocholine (POPC), 1,2-dioleoyl-*sn*-glycero-3-phosphocholine (DOPC), 1,2-dipetroselinoyl-*sn*-glycero-3-phosphocholine (PCΔ6) and 1,2-dioleoyl-*sn*-glycero-3-phospho(Tempo)choline (TEMPO) were supplied by Avanti Polar Lipids (Alabaster, AL, USA). 6-Hexadecanoyl-2-(((2-(trimethylammonium)ethyl)methyl)amino) naphthalene chloride (Patman) was purchased from Molecular Probes (Eugene, OR, USA) and used without further purification. Spin-labeled quenchers, 2-(3-carboxypropyl)-4,4-dimethyl-2-tridecyl-3-oxazolidinyloxy (5-doxyl-stearic acid) and 2-(14-carboxytetradecyl)-2-ethyl-4,4-dimethyl-3-oxazolidinyloxy (16-doxyl-stearic acid) and D_2O were obtained from Aldrich (Steinheim, Germany). Acrylamide and Tris were ordered from Fluka (Buchs, Switzerland). Solvents of spectroscopic grade were supplied by Merck (Darmstadt, Germany).

2.2. Sample preparation for the SR measurements

Lipid in chloroform and dye in methanol were mixed with a 100:1 lipid to dye molar ratio. The organic solvents were removed under the stream of nitrogen and lipids were rehydrated with Tris buffer (50 mM Tris, pH 7.4, 100 mM NaCl) in order to obtain 1 mM lipid concentration (except for quenching with spin-labeled compounds and acrylamide, where 0.2 and 0.08 mM lipid concentrations were used, respectively). LUVs were prepared by the extrusion with polycarbonate filters (100 nm pore diameter). Samples for parallax method quenching were prepared by mixing appropriate spin-labeled compound with the lipid solution before evaporation to obtain 15 mol% of final concentration of quencher. Prepared samples were transferred to 1 cm quartz cuvette and equilibrated at desired temperature for 10 min before each measurement.

2.3. Steady-state fluorescence measurements

All steady-state excitation and emission spectra were performed with Fluorolog-3 spectrofluorometer (model FL3-11, Jobin Yvon Inc., Edison, NJ, USA) equipped with Xenon-arc lamp. Spectra were collected with 1 nm steps (2 nm bandwidths). Temperature was maintained within ± 0.1 K with a water-circulating bath.

2.4. Fluorescence quenching with acrylamide

Fluorescence intensity after serial addition of small aliquots of a stock solution of 5 M acrylamide in water to a stirred sample was measured at the maximum of emission spectrum. The excitation wavelength used was 373 nm. Quenching data were fitted to the Stern–Volmer equation (Lakowicz, 1999)

$$\frac{F_0}{F} = 1 + K_D[Q], \quad (1)$$

where F_0 and F are the fluorescence intensities in the absence and presence of quencher, respectively, K_D the Stern–Volmer quenching constant and $[Q]$ is the concentration of quencher.

2.5. Parallax fluorescence quenching

Parallax analysis of fluorescence quenching (Abrams and London, 1993; Chattopadhyay and London, 1987) was used to determine membrane penetration depths for the fluorescence dyes used. The steady-state fluorescence intensity as well as fluorescence decays were measured at different wavelengths from the emission range for the samples with and without quencher. Data collected for the three quenchers used were analyzed in pairs to obtain the distance h of the dye from the bilayer

center according to (Abrams and London, 1993):

$$h = \frac{\pi C(h_{q1}^2 - h_{q2}^2) - \ln(F_1/F_2)}{2\pi C(h_{q1} - h_{q2})}, \quad (2)$$

F is the fluorescence intensity in the presence of quencher, and h_q is the distance of the quencher from the center of the bilayer. The 1 and 2 subscripts indicate shallower and deeper quenchers, respectively. C is the surface concentration of the quencher in molecules per unit area.

The results obtained with different pairs of the quenchers were compared.

An alternative method to obtain fluorophore position is to calculate the distribution function of the quenched dye by fitting the data collected for all three quenchers with the parallax profile:

$$\ln\left(\frac{F_0}{F(h_q)}\right) = \begin{cases} \pi C[R_c^2 - (h_q - h)^2] & : \ h_q - h < R_c \\ 0 & : \ h_q - h \geq R_c \end{cases}, \quad (3)$$

where $F(h_q)$ is the fluorescence intensity in the presence of the quencher located at distance h_q from the bilayer center and R_c is the radius of quenching (Thoren et al., 2004). In the present work, both methods were used for the comparison.

2.6. Time-resolved fluorescence measurements

Fluorescence decays were recorded on a 5000U Single Photon Counting equipment (IBH, Glasgow, UK) using an IBH laser diode NanoLED 11 (370 nm peak wavelength, 80 ps pulse width, 1 MHz maximum repetition rate) and a cooled Hamamatsu R3809U-50 microchannel plate photomultiplier. Emission decays were recorded at a series of wavelengths spanning the steady-state emission spectrum (400–540 nm) with 10 nm steps. All measurements were recorded with same emission slits setup (8 nm bandwidths) at magic angle. Additionally, 399 nm cutoff filter was used to eliminate scattered light. The signal was kept below 2% of the light source repetition rate (1 MHz). The time resolution of the experimental setup, calculated as 1/5 of full width of half maximum (FWHM) of instrument response function, was about 16 ps. Fluorescence decays were fitted to multi-exponential functions (two or three exponential components were used) using the iterative reconvolution procedure with the IBH DAS6 software.

2.7. Solvent relaxation technique

Methodology used in our laboratory to study relaxation of hydrated lipid bilayers has been already described in details in a few reviews (Hof, 1999; Hutterer et al., 1998; Jurkiewicz et al., 2005; Sykora and Hof, 2002). Herein, only the general principles of the method are outlined.

The time-resolved emission spectra (TRES) were obtained by the spectral reconstruction method (Horng et al., 1995) and fitted by the log–normal function in order to determine spectra position $\nu(t)$ (in terms of their maxima) and the full width at half maximum (FWHM). The spectral response function (or relaxation function) defined as:

$$C(t) = \frac{\nu(t) - \nu(\infty)}{\nu(0) - \nu(\infty)} = \frac{\nu(t) - \nu(\infty)}{\Delta\nu}, \quad (4)$$

was calculated using the position of estimated time-zero spectrum as $\nu(0)$. This so-called time-zero spectrum is the hypothetical fluorescence spectrum emitted by the vibrationally relaxed dye prior to any solvent motions occurred. It cannot be measured directly in most systems due to finite temporal resolution of the apparatus, however, it can be estimated using absorption and steady-state emission spectra measured in the non-polar solvents as was described previously (Fee and Maroncelli, 1994). Comparison of the positions of the estimated time-zero spectrum and of the very first spectrum gained by the spectral reconstruction also allows determination of the percentage of the solvation process that is captured by the method.

To numerically characterize solvent relaxation process two parameters were calculated. First one, $\Delta\nu$ is the overall emission shift, which was shown to be directly proportional to the polarity function of a solvent, in which the dye is dissolved (Horng et al., 1995). In case of the relaxation in phospholipid/water, where the polarity is attributed to the water molecules, the $\Delta\nu$ parameter reflects mainly the amount of hydration of the bilayer at the level, where the dye is located. The second information obtained from the analysis of the TRES is the kinetics of solvation being proportional to the viscosity of the probed dye microenvironment (Richert et al., 1994). The time course of the $C(t)$ might be expressed in several ways (Horng et al., 1995). Here, we use the so-called integral solvent relaxation time which is defined as the area under the $C(t)$ curve:

$$\tau_r = \int_0^\infty C(t)\,dt \quad (5)$$

2.8. Sample preparation for NMR studies

The appropriate amount of lipid was dried in vacuum at room temperature for 24 h. The lipid film was then hydrated with Tris buffer (50 mM Tris, pH 7.4, 100 mM

NaCl in D_20) to obtain 6–20 D_2O molecules per lipid. Fifty milligrams of sample were sealed in glass tubes and homogenized by five freeze–thaw cycles followed by centrifugation and stored at 298 K for 24 h.

2.9. NMR method

The ^{2}H-spectra were recorded on a Chemagnetics Infinity 100 spectrometer (Fort Collins, USA) at 15.37 MHz. A standard quadrupole echo pulse sequence ($\pi/2$-τ-$\pi/2$-τ-acquisition) was used with an interpulse delay τ of 50 μs. The 90° pulse length was 6 μs (OPPC, POPC) and 7 μs (DOPC) with a repetition time of 1 s. Experiments were carried out at 298 and 318 K.

3. Results and discussion

3.1. Location of Patman in DOPC, OPPC, POPC and PCΔ6 LUVs

Precise determination of the location of fluorescent probe and its stability within the membrane was found to be a prerequisite for the correct SR data analysis (Jurkiewicz et al., 2006). The issue is discussed here in detail.

The application of parallax quenching method allows determining the location of the fluorophore in the membrane. The value of the distance from the bilayer center obtained recently for Patman calculated according to Eq. (2) was 10.4 Å (Jurkiewicz et al., 2006). The distributional fitting (Eq. (3)) confirms this result, additionally providing a measure of how broad the distribution may be. However, the distribution obtained in this way includes not only the distribution of the dye location itself, but is also affected by the distributions of quenchers' positions as well as other processes that influence quenching ratios (e.g. molecular motions) (Abrams and London, 1992). Indeed, the doxyl labeled lipids were shown to be relatively broadly distributed in the membrane, and thus the values obtained using the parallax analysis should be seen as mean locations (Vogel et al., 2003). It was already presumed, when introducing parallax method that the calculated distances result from the averaging over a couple of angstroms (Chattopadhyay and London, 1987). Nevertheless, the method has proved to be of great importance for SR data analysis and fluorescent probes comparison.

The position calculated for Patman was obtained from single wavelength measurement (emission maximum at 475 nm); although, a systematic dependence of calculated position on the chosen emission wavelength was observed. This dependence can be a source

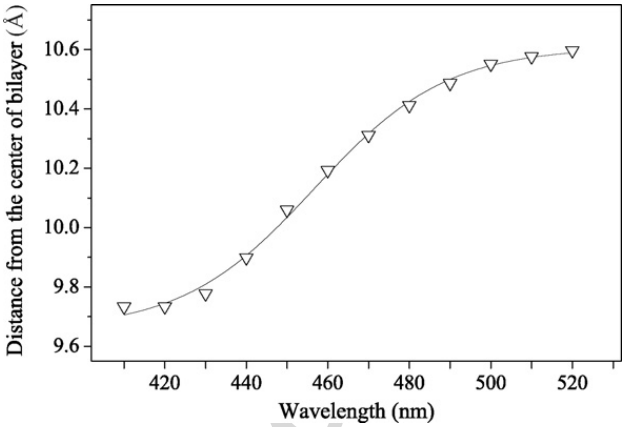

Fig. 1. The distribution of the location of Patman within a DOPC bilayer as obtained in (Jurkiewicz et al., 2006). Distance of the dye from the centre of the DOPC bilayer was calculated for different emission wavelengths, according to Eq. (2). Measurements performed at 293 K for excitation at 373 nm. The data points are fitted with sigmoidal function (solid line).

of valuable information about the distribution of the fluorophore location; particularly for the membrane fluorescent polarity probes. This is because of the strong polarity gradient (caused predominantly by hydration) along the membrane normal. Since the gradient is especially steep in the region, where the Patman is located, and the Stokes-shift of the dye depends on the polarity, the wavelength dependent parallax curve characterizes the range of Patman location. In the case of Patman embedded into DOPC bilayer this range was found to be <1 Å (Jurkiewicz et al., 2006), which is considerably small in comparison with the length of the chromophore of about 7 Å (Ilich and Prendergast, 1989; Parusel et al., 1998). It is important to stress the fact that due to all previously mentioned uncertainties, the values obtained by parallax method, including the wavelength dependent distribution, are averages and that the real values can vary (Fig. 1).

Acrylamide is commonly used to determine the relative depths of membrane penetration by proteins and fluorescent dyes. In our work, acrylamide quenching pro-

Table 1
The quenching of Patman embedded in DOPC, OPPC, POPC and PCΔ6 LUVs with acrylamide titrated to the buffer

Lipid	K_D (M^{-1})
DOPC	0.26 ± 0.01
OPPC	0.27 ± 0.01
POPC	0.28 ± 0.01
PCΔ6	0.27 ± 0.01

K_D, Stern–Volmer constants as defined by Eq. (1) and calculated by fitting the data points to a straight line. Measurements performed at 293 K, excitation and emission wavelengths 373/450 nm, respectively.

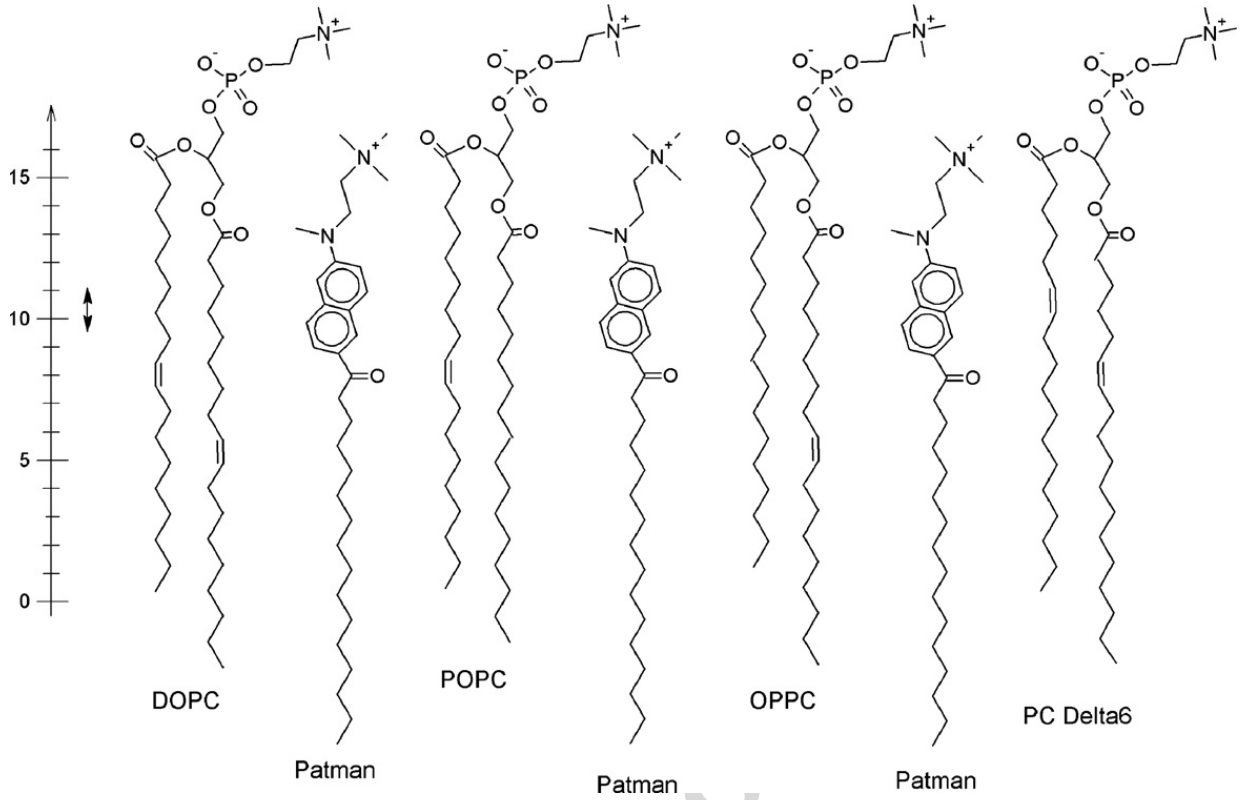

Fig. 2. Schematic illustration of the location of Patman within lipid bilayer composed of DOPC, POPC, OPPC and PCΔ6. The scale on the left shows the approximate distance from the centre of the bilayer. Double-sided arrow indicates distribution of the fluorophore of Patman in the membrane.

vided information whether in all four investigated lipid systems (DOPC, OPPC, POPC and PCΔ6), the chromophore of Patman is located at the same distance from the lipid–water interface. As presented in Table 1, the acrylamide quenching experiments show no significant differences for the four lipids studied. Thus, the obtained location of the chromophore can be deduced to be very similar in all measured systems (Fig. 2). We can conclude that the chromophore of Patman is located slightly below the level of the hydrated ester-group of the *sn*-1 lipid chain and that the depth of location is not changed by the chemical nature of the acyl chains. Even though some relocation of Patman have been found in case of cationic lipid membranes (Jurkiewicz et al., 2006), for the electrically neutral lipids, like the ones studied here, Patman seems to be the dye of choice for SR studies due to its precise, unimodal and highly stable location.

3.2. SR experiments in DOPC, OPPC, POPC and PCΔ6 LUVs

It was shown that the solvation dynamics in lipid bilayers becomes faster with increasing temperature (Hutterer et al., 1997). This trend is visible when comparing the SR characteristics in a particular bilayers system at different temperatures (see Table 2). Trivially increasing temperature leads to higher headgroup mobility. On the other hand, in all four investigated lipid systems the $\Delta\nu$ values are invariant with the temperature, indicating that the level of hydration in the vicinity of the chromophore does not change within the examined temperature range.

When comparing lipids with different phase transition temperatures (T_m), the measurements are often performed at certain temperature offset above that phase

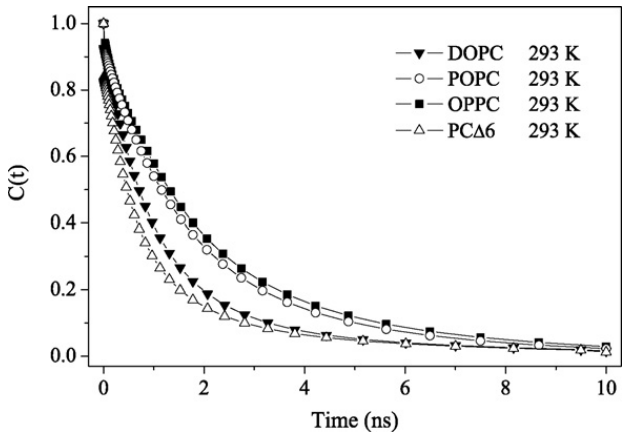

Fig. 3. Correlation functions for Patman in DOPC (▼), POPC (◯), OPPC (■) and PCΔ6 (△) LUVs. Measurements were performed at 293 K.

Table 2
Characteristics of the solvent relaxation process in POPC, OPPC, DOPC and PCΔ6 liposomes probed by Patman at 283 and 298 K

Lipid	283 K			298 K		
	$\Delta\nu$ (cm^{-1})[a]	τ_r (ns)[b]	Observed (%)[c]	$\Delta\nu$ (cm^{-1})[a]	τ_r (ns)[b]	Observed (%)[c]
POPC	3400	3.43	94	3500	1.73	94
OPPC	3400	3.69	96	3450	1.81	93
DOPC	3500	1.98	96	3500	1.23	91
PCΔ6	3500	1.56	89	3500	1.04	86

[a] $\nu = \nu(0) - \nu(\infty)$; $\nu(0)$ – estimated (see text); $\nu(\infty)$ – obtained from the reconstructed TRES.
[b] Integral average relaxation time calculated according to Eq. (5).
[c] Percentage of the observed SR process obtained by comparing $\Delta\nu$ values calculated using the estimated $\nu(0)$ and the $\nu(0)$ obtained exclusively from TRES reconstruction.

transitions of these lipids (at the so-called relative temperatures). It is also assumed that at the certain temperature (above T_m of both compared lipids) the dynamics of the lipid with lower T_m should be faster. This assumption holds true, when comparing the DOPC with either POPC or OPPC at both 283 and 298 K (Table 2). Considering the T_m values of those lipids (Koynova and Caffrey, 1998) it is understandable that the SR curves for DOPC ($T_m = 254.8 \pm 3.6$ K) decreases considerably faster than both for POPC ($T_m = 270.6 \pm 2.4$ K) and OPPC ($T_m = 264.2 \pm 0.7$ K) (Fig. 3). Surprisingly, when the OPPC and POPC isomers are compared, the faster relaxation is observed for POPC, which is closer to its phase transition temperature (Fig. 3 and Table 2). The difference in the solvent relaxation kinetics between OPPC and POPC becomes even more evident when measured in the temperatures relative to the phase transition (see Fig. 4). In this case (OPPC measured at 294 K and POPC measured at 301 K; in other words 30 K above their phase transitions) the difference in the relaxation times between the two lipids reaches 30%. We attribute these results to the different depth of double bond position in the POPC and OPPC bilayers. The double bond containing chain in POPC is attached at the *sn*-2 position, which is located closer to the water phase (see Fig. 2) than the *sn*-1 (which is the attaching point for OPPC double bond containing chain). Thus, in POPC the double bonds are located closer to the glycerol level, where the Patman resides, which explains why the faster SR kinetics is observed.

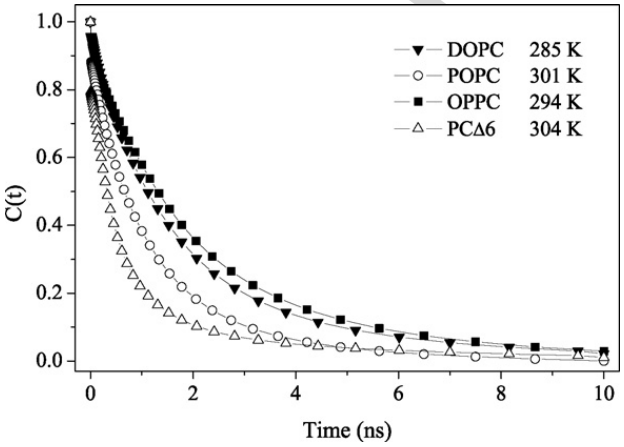

Fig. 4. Correlation functions for Patman in DOPC (▼), POPC (◯), OPPC (■) and PCΔ6 (△) LUVs. Measurements were performed at temperatures relative to the transition temperatures T_m of the lipids.

In order to investigate the influence of the position of the double bonds within the acyl chains on the solvent relaxation kinetics of Patman, measurements in PCΔ6 liposomes were performed. While DOPC contains double bonds at 9th carbons, in PCΔ6 the double bonds are shifted three carbons up to the 6th carbons positions, which results in a substantial increase of the main phase transition temperature from 254.8 to 274.2 K (Koynova and Caffrey, 1998). When measuring DOPC and PCΔ6 at 283 K at which the systems are 28 and 9 K above their phase transition temperatures, respectively, one should again expect a substantially faster kinetics in the DOPC membrane. However, the obtained relaxation times τ_r present opposite trends for 283 K as well as for 298 K (Table 2). The τ_r decreases from 1.98 ns for DOPC to 1.56 ns for PCΔ6 at 283 K and from 1.23 to 1.04 ns at 298 K. It is worth noticing that SR kinetics at 283 K for PCΔ6 is also much faster than for both POPC and OPPC, even though the T_m of PCΔ6 is the highest. The comparison of SR kinetics in these lipids gives clear evidence that the mobility of the hydrated lipid molecules is not only the function of the lipid phase transition temperature. The water molecules bound to the ester-groups probed by Patman are apparently more mobile if the double bonds disturbing lipid packing are located closer to the phospholipid headgroups.

Regarding the level of hydration of the membranes represented by the $\Delta\nu$ parameter we observe a difference at 283 K between OPPC and POPC on one side and

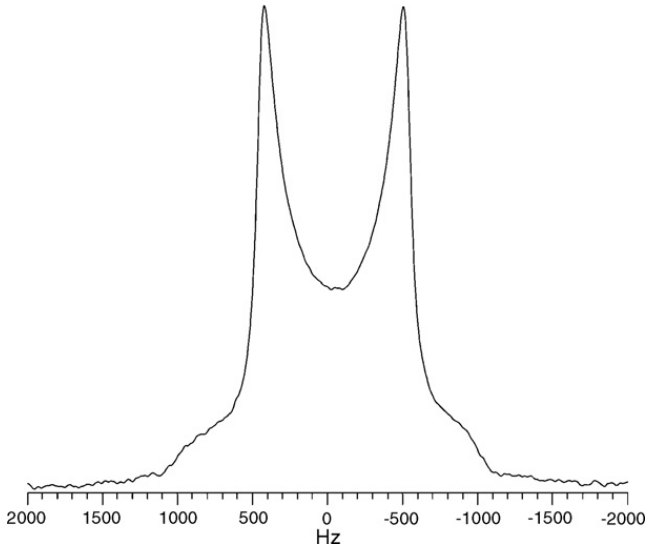

Fig. 5. ^{2}H NMR line shape of D_2O in multilamellar OPPC vesicles at 298 K with a hydration level of nine water molecules per lipid. The characteristic ^{2}H NMR quadrupole splitting is around 930 Hz.

DOPC and PCΔ6 on the other side (Table 2). By the level of hydration or the hydration itself we understand here the number of water molecules present in the vicinity of the probe chromophore. In this case, the water molecules are predominantly bound to the lipids. The ester-groups probed by Patman are apparently more hydrated in the case of DOPC and PCΔ6, which possess double unsaturated fatty acid chains. These hydration changes are less detectable at higher temperatures and at 298 K they are already within the experimental error (50 cm^{-1}). The $\Delta\nu$ values are in general agreement with SR kinetics (i.e. the larger the $\Delta\nu$ the smaller the τ_r), which means that the increased hydration of the membrane also increases its mobility. The kinetics is, however, much more sensitive to the different lipids studied in this work.

3.3. NMR results

Wide line static ^{2}H NMR spectra were obtained for multilamellar vesicles composed of either POPC, OPPC, or DOPC under variation of the hydration degree (water to lipid ratio, *R*) and temperature. In Fig. 5, a typical NMR spectrum is displayed for OPPC vesicles at 298K upon hydration with nine heavy water molecules per lipid. The NMR spectrum is typical for lipid bilayers in their liquid-crystalline phase where the water molecules in the first lipid hydration shells undergo fast anisotropic reorientation (Sparrman and Westlund, 2003; Aman et al., 2003). Due to the low hydration degree no exchange with free water molecules can occur and therefore no isotropic NMR lines are visible but a residual quadrupole NMR spectrum is observed with its typical powder peak shape which displays a quadrupole splitting of $\Delta\nu Q = 930$ Hz between the two main resonance peaks. This characteristic quadrupole splitting, $\Delta\nu Q$ provides information about the different fractions of water molecules hindered by the interactions at the lipid–water interface (Aman et al., 2003; Sparrman and Westlund, 2003). However, the NMR spectrum does not reflect a single population of water molecules but rather the time-average of two water hydration pools which are in fast exchange with each other, as recently described (Aman et al., 2003; Sparrman and Westlund, 2003). The first hydration pool exhibits a positive order parameter for the water molecules situated near the headgroup region (Aman et al., 2003). This water population is in fast exchange with a second pool of water molecules located at the glycerol and upper fatty acid region. There, the water molecules have a negative order parameter due to their different time-averaged orientation with respect to the membrane normal in comparison to the first water pool. These two water populations have different NMR spectra (different quadrupole splittings). However, due to the fast exchange rate only a time-averaged NMR spectrum can be seen with a single quadrupole splitting.

Nevertheless, the change in the ratio between these two water populations, affects the NMR spectrum; i.e. the increased population of water situated in the hydrophobic part results in larger observable quadrupole

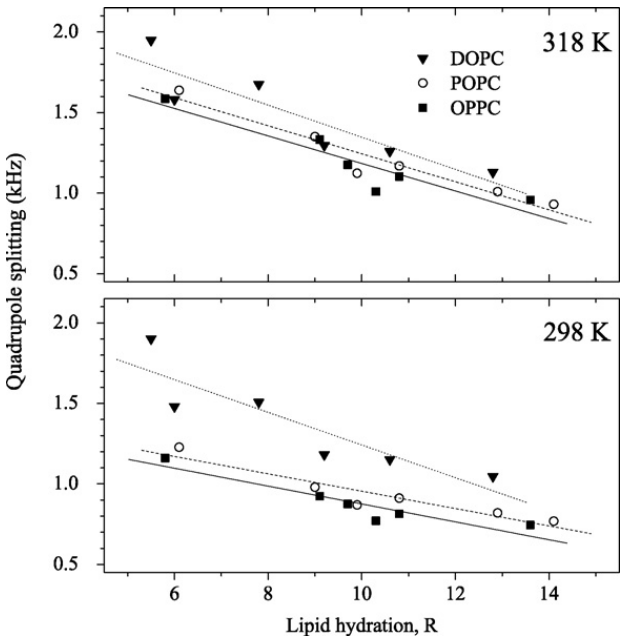

Fig. 6. ^{2}H quadrupole splittings and the corresponding linear fits for D_2O in hydrated OPPC (■, solid line), POPC (◯, dashed line) and DOPC (▼, dotted line) vesicles at 298 K (top) and 318 K (bottom) with lipid hydration ranging from 5 to 14 water molecules per lipid.

splitting (Aman et al., 2003; Sparrman and Westlund, 2003). This behavior is clearly visible in Fig. 6, where the obtained values for the quadrupole ^2H splittings for D_2O in lipid vesicles are plotted against the hydration ratio R. For all ratios, the quadrupole splitting for DOPC is significantly larger than the one obtained for the other two lipids (e.g. for $R = 9$, the obtained splitting is increasing from 930 Hz for OPPC and 980 Hz for POPC to 1180 Hz for DOPC). Clearly, DOPC has the highest fraction of water situated in its hydrophobic part compared to POPC and OPPC. Inspecting the molecular structure of these lipids (Fig. 2), it is understandable that in the case of DOPC the two unsaturated fatty acid chains increase the disorder in the upper part of the hydrophobic region of the lipid bilayer. This increased disorder (also determined by NMR (Warschawski and Devaux, 2005) and visible by the SR results) enables a deeper penetration of water molecules into the glycerol and fatty acid region. As a result, the number of water molecules with negative order parameter increases, which is reflected in an increased NMR quadrupole splitting. Opposite to DOPC, both POPC and OPPC have only one unsaturated fatty acid chain. Therefore, the lipid molecules are more tightly packed in their hydrophobic region, which prevents water molecules from penetrating deeper into the bilayer. This is reflected in a reduced value of the quadrupole splitting. The differences between POPC and OPPC at 298 K, although visible in Fig. 6, are very small and thus their agreement with SR kinetics results is not definite.

Increasing the temperature induces a higher disorder into the bilayer hydrophobic core for all three lipids, which is reflected by increased isomerization rates of the various chain segments (Warschawski et al. 2005; Weisz et al., 1992). Therefore, the hydrophobic packing near the glycerol region is further reduced, enabling even more water molecules to penetrate into the hydrophobic region. This phenomenon occurs, as expected in all three lipid bilayers, as visible into increased quadrupole splittings in the corresponding NMR spectra upon an increase of temperature (Fig. 6).

4. Conclusions

Comparison of SR results obtained for DOPC, POPC, OPPC and PCΔ6 shows that not only the relative temperature to the phase transition temperature influences the mobility in the membrane, but also the position of the double bond in the acyl chain. The closer the double bond is to the *sn*-1 ester-group, the more mobile this group is. Both SR $\Delta\nu$ parameter and NMR quadrupole splitting results indicate increased hydration of phosphocholines with double unsaturated fatty acid chains in comparison with those with only one unsaturated chain. These hydration changes, also for both techniques, become less visible at higher temperatures, where the mobility of the hydrated lipid groups becomes faster as reflected in the SR kinetics. The NMR and SR provide important information about membrane hydration and mobility of hydrated groups being rather complementary than competitive methods.

The evaluation of the probe location and its stability in all measured systems is a precondition for the correct interpretation of the SR results (which holds true for many other fluorescence techniques). According to this, Patman is the dye of choice for SR studies of electrically neutral lipids due to its precise location within the lipid bilayer.

Acknowledgements

Financial support of the Czech Academy of Sciences via A400400503 (M.H.), the Czech Science Foundation (GACR) via 203/05/2308 (A.Z.) and via 203/05/H001 (A.O.), the Ministry of Education, Youth and Sports of the Czech Republic via LC06063 (P.J., J.S.) and the Swedish Research Council via 621-2001-3185 (G.G.) is gratefully acknowledged.

References

Abrams, F.S., London, E., 1992. Calibration of the parallax fluorescence quenching method for determination of membrane penetration depth—refinement and comparison of quenching by spin-labeled and brominated lipids. Biochemistry 31, 5312–5322.

Abrams, F.S., London, E., 1993. Extension of the parallax analysis of membrane penetration depth to the polar-region of model membranes—use of fluorescence quenching by a spin-label attached to the phospholipid polar headgroup. Biochemistry 32, 10826–10831.

Aman, K., Lindahl, E., Edholm, O., Hakansson, P., Westlund, P.O., 2003. Structure and dynamics of interfacial water in an L-alpha phase lipid bilayer from molecular dynamics simulations. Biophys. J. 84, 102–115.

Chattopadhyay, A., London, E., 1987. Parallax method for direct measurement of membrane penetration depth utilizing fluorescence quenching by spin-labeled phospholipids. Biochemistry 26, 39–45.

Fee, R.S., Maroncelli, M., 1994. Estimating the time-zero spectrum in time-resolved emission measurements of solvation dynamics. Chem. Phys. 183, 235–247.

Hof, M., 1999. Solvent relaxation in biomembranes. In: Rettig, W., Strehmel, B., Schrader, S. (Eds.), Applied Fluorescence in Chemistry, Biology, and Medicine. Springer Verlag, Berlin, pp. 439–456.

Horng, M.L., Gardecki, J.A., Papazyan, A., Maroncelli, M., 1995. Subpicosecond measurements of polar solvation dynamics—coumarin-153 revisited. J. Phys. Chem. 99, 17311–17337.

Hutterer, R., Parusel, A.B.J., Hof, M., 1998. Solvent relaxation of Prodan and Patman: a useful tool for the determination of polarity and rigidity changes in membranes. J. Fluoresc. 8, 389–393.

Hutterer, R., Schneider, F.W., Hof, M., 1997. Time-resolved emission spectra and anisotropy profiles for symmetric diacyl- and diether-phosphatidylcholines. J. Fluoresc. 7, 27–33.

Hutterer, R., Schneider, F.W., Sprinz, H., Hof, M., 1996. Binding and relaxation behaviour of Prodan and Patman in phospholipid vesicles: a fluorescence and H-1 NMR study. Biophys. Chem. 61, 151–160.

Ilich, P., Prendergast, F.G., 1989. Singlet adiabatic states of solvated Prodan—a semiempirical molecular-orbital study. J. Phys. Chem. 93, 4441–4447.

Jurkiewicz, P., Olzynska, A., Langner, M., Hof, M., 2006. Headgroup hydration and mobility of DOTAP/DOPC bilayers: a fluorescence solvent relaxation study. Langmuir 22, 8741–8749.

Jurkiewicz, P., Sykora, J., Olzynska, A., Humplickova, J., Hof, M., 2005. Solvent relaxation in phospholipid bilayers: principles and recent applications. J. Fluoresc. 15, 883–894.

Koynova, R., Caffrey, M., 1998. Phases and phase transitions of the phosphatidylcholines. Biochim. Biophys. Acta 1376, 91–145.

Lakowicz, J.R., 1999. Principles of Fluorescence Spectroscopy. Kluwer Academic/Plenum Press, New York, NY.

Lakowicz, J.R., Bevan, D.R., Maliwal, B.P., Cherek, H., Balter, A., 1983. Synthesis and characterization of a fluorescence probe of the phase-transition and dynamic properties of membranes. Biochemistry 22, 5714–5722.

Nilsson, L., Halle, B., 2005. Molecular origin of time-dependent fluorescence shifts in proteins. Proc. Natl. Acad. Sci. U.S.A. 102, 13867–13872.

Parusel, A.B.J., Nowak, W., Grimme, S., Kohler, G., 1998. Comparative theoretical study on charge-transfer fluorescence probes: 6-propanoyl-2-(*N*,*N*-dimethylamino)naphthalene and derivatives. J. Phys. Chem. A 102, 7149–7156.

Richert, R., Stickel, F., Fee, R.S., Maroncelli, M., 1994. Solvation dynamics and the dielectric response in a glass-forming solvent—from picoseconds to seconds. Chem. Phys. Lett. 229, 302–308.

Sparrman, T., Westlund, P.O., 2003. An NMR line shape and relaxation analysis of heavy water powder spectra of the L-alpha, L-beta 'and P-beta' phases in the DPPC/water system. Phys. Chem. Chem. Phys. 5, 2114–2121.

Sykora, J., Hof, M., 2002. Solvent relaxation in phospholipid bilayers: physical understanding and biophysical applications. Cell. Mol. Biol. Lett. 7, 259–261.

Sykora, J., Kapusta, P., Fidler, V., Hof, M., 2002. On what time scale does solvent relaxation in phospholipid bilayers happen? Langmuir 18, 571–574.

Thoren, P.E.G., Persson, D., Esbjorner, E.K., Goksor, M., Lincoln, P., Norden, B., 2004. Membrane binding and translocation of cell-penetrating peptides. Biochemistry 43, 3471–3489.

Vogel, A., Scheidt, H.A., Huster, D., 2003. The distribution of lipid attached spin probes in bilayers: application to membrane protein topology. Biophys. J. 85, 1691–1701.

Warschawski, D.E., Devaux, P.F., 2005. Order parameters of unsaturated phospholipids in membranes and the effect of cholesterol: a 1H–13C solid-state NMR study at natural abundance. Eur. Biophys. J. 34, 987–996.

Weisz, K., Grobner, G., Mayer, C., Stohrer, J., Kothe, G., 1992. Deuteron nuclear-magnetic-resonance study of the dynamic organization of phospholipid cholesterol bilayer-membranes—molecular-properties and viscoelastic behavior. Biochemistry 31, 1100–1112.